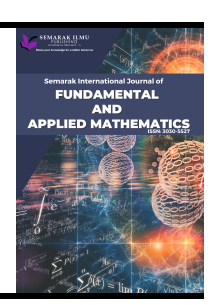


Semarak International Journal of Fundamental and Applied Mathematics

Journal homepage: https://semarakilmu.my/index.php/sijfam ISSN: 3030-5527



Robust Epidemic Mitigation Algorithm: Real-Time Parameter Calibration and Multi-Scenario Optimization for Vaccination

Saratha Sathasivam^{1,*}, Muraly Velavan², Sabastine Emmanuel³, Emmerline Shelda Siaw⁴, Aceng Sambas⁵

- $^{\, 1}$ School of Mathematical Sciences, Universiti Sains Malaysia, 11800 USM, Penang, Malaysia
- School of General and Foundation Studies, AIMST University, 08100 Semeling, Malaysia
- ³ Department of Mathematics, Federal University Lokoja, Kogi State, Nigeria
- Centre for Pre-University Studies Universiti Malaysia Sarawak 94300 Kota Samarahan, Sarawak, Malaysia
- ⁵ Universitas Muhammadiyah Tasikmalaya, Tasikmalaya, 46196, Indonesia

ARTICLE INFO

ABSTRACT

Article history:

Received 3 October 2025 Received in revised form 27 October 2025 Accepted 29 October 2025 Available online 3 November 2025

Vaccination and control methods in areas prone to outbreaks, like Malaysia, must be guided by accurate mathematical models of infectious illnesses. This work introduces a revised Susceptible-Infectious-Recovered (SIR) model that accounts for changing public health responses by including time-dependent immunization. Aiming to reduce implementation costs and infection levels in the face of uncertainty, the model seeks to identify optimal vaccination regimens. To validate the model and estimate parameters, we use influenza incidence data from 2015 to The model is solved and analyzed using two numerical methods, which are compared in terms of computing efficiency, convergence behavior, and stability across different parameter values. In order to determine how changes in transmission and control rates affect important epidemiological variables, including basic reproduction number, epidemic peak, and final infection size, a sensitivity analysis is conducted. In comparison to static tactics, the results demonstrate that adaptive vaccination controls are more effective in reducing the spread of epidemics. A dependable foundation for developing data-driven, cost-effective epidemic management plans may be found in the study's demonstration of the synergy between optimal control principles and resilient numerical approaches. The real-time control of influenza transmission in Malaysia is much improved by this integration, which also improves the accuracy of the models.

Keywords:

Epidemic model; finite difference method; influenza modelling letters

1. Introduction

Infectious diseases have long been a significant and persistent threat to public health [1,2]. In recent years, the importance of epidemiological models in predicting and controlling the spread of infectious diseases has become increasingly evident, particularly in the context of global health challenges such as the COVID-19 pandemic and seasonal influenza outbreaks [2,3]. Influenza remains

E-mail address: saratha@usm.my

https://doi.org/10.37934/sijfam.8.1.5570

55

^{*} Corresponding author.

a significant public health concern in Malaysia. According to the World Health Organisation, Malaysia experienced a notable increase in influenza-like illness cases in late 2024, with weekly rates reaching 73.9 per 1,000 outpatient visits. Historical surveillance data from 2015 to 2018 recorded over 11,000 cases of influenza-like illness, highlighting seasonal and subtype variations that emphasize the ongoing burden of this disease [4-6].

Worldwide, infectious diseases remain major public health concerns, necessitating the use of mathematical models to inform intervention and policy efforts. One of the most essential models in epidemiology for understanding disease dynamics and explaining the transmission of communicable illnesses within populations is the Susceptible-Infectious-Recovered (SIR) model, introduced by Kermack and McKendrick in 1927 [7,8]. It has become a vital tool for studying epidemics, whether seasonal illnesses like influenza or new outbreaks such as COVID-19, thanks to its simplicity and ease of use. Traditional SIR models fall short when it comes to public health measures like vaccination, quarantine, and behavioural changes because they assume homogeneous mixing and fixed characteristics. Modified SIR frameworks incorporate time-dependent controls, including vaccination efforts, which enable the modelling of real-world scenarios. Vaccination rates may change over time due to factors such as public compliance, logistics, and availability. A solid mathematical foundation for developing immunisation programmes that reduce disease burden while balancing resource limitations is provided by optimal control theory, particularly through Pontryagin's Maximum Principle (PMP) [9,10].

Many infectious disease models use the SIR model diagram. It illustrates how humans progress through the Susceptible, Infectious, and Recovered compartments. It works for lifelong-immune illnesses, including measles and seasonal influenza. The SEIR model includes an Exposed (E) compartment between susceptible and infectious individuals for latent illnesses, such as COVID-19 or Ebola, to describe the delay between infection and infectiousness. SIRS permits recovered individuals to become vulnerable again, making it suited for studying recurring epidemics and vaccine-induced immunity loss. Death (D) compartments in the SIRD model track disease-induced deaths, essential for high-fatality epidemics. A vaccination control mechanism in the SIRV model allows susceptible individuals to transition into the recovered class. This approach enables public health planners to assess time-dependent vaccination strategies, identify appropriate control methods, and evaluate cost-benefit trade-offs. To evaluate containment and contact tracing, complex diagrams such as the SIQR or SEIQR isolate infected or exposed individuals from the general population in quarantine compartments.

To determine the optimal vaccination rate that minimizes the number of infectious individuals and the economic cost of vaccination over a finite time horizon, we formulate an optimal control problem in this work. A bounded control function represents the vaccination rate v(t) in the updated SIR model, which is subject to real-world constraints. A system of nonlinear ODEs governs the system, and PMP is used to derive the optimal control method. To measure how well the control intervention worked, the necessary epidemiological measures, including the basic reproduction number a_0 , peak infection, and final epidemic size, are also taken into account. In most cases, solving these controlled ODE systems analytically is very challenging; therefore, numerical approaches are often used instead. In this study, we apply and evaluate two computing methods: the Differential Transformation Method (DTM) and the Finite Difference Method (FDM). DTM, a semi-analytical approach based on Taylor series expansions, provides excellent accuracy at a low computational cost [11-13]. In contrast, FDM is a classical discretization technique renowned for its dependability and ease of implementation. By contrasting FDM with DTM, we can evaluate their stability, accuracy, and computational efficiency in solving the controlled epidemic model.

The environment of influenza transmission in Malaysia provides a valuable case study because of the country's dense population, frequent flu seasons, and availability of vaccine programs [14, 15]. Numerical assessment of control impacts, verification of convexity of the Hamiltonian for optimality sufficiency, and sensitivity analysis on essential parameters (e.g., recovery and transmission rates, cost weights) are all part of the study. To inform dynamic and resource-sensitive vaccination programs, this research integrates optimal control theory with efficient numerical methods. As a whole, it adds to computational epidemiology. The findings can help health officials in Malaysia and other nearby areas to plan for and respond to seasonal or unexpected infectious disease outbreaks cost-effectively and efficiently [16].

Malaysia was chosen for its surveillance and vaccine capacity to research influenza dynamics. Develop an Adaptive Optimal Epidemic Control (AOEC) method to optimise vaccinations under uncertainty. We suggest a multi-year (2024–2027) SIRU model with declining immunity, variable vaccination, and time-dependent transmission. The Extended Kalman Filter provides a real-time estimate with adaptive parameter updates and robust scenario optimization. By revealing vaccination schedules that are cost-efficient during seasonal epidemics, the suggested framework can assist Malaysia's Ministry of Health. In order to prioritize high-risk areas and maximize vaccine allocation during periods of limited availability, public health authorities can use real-time infection data to change vaccination timing.

2. Methodology

From 2015 to 2025, the model will simulate the transmission of influenza in Malaysia. The model is expanded to include a constant vaccination rate (μ) to reduce the susceptible population over time. The SIR model with vaccine differential equations is:

$$\frac{dS}{dt} = -\frac{\beta(t)SI}{N} - \mu(t)S \tag{1}$$

$$\frac{dI}{dt} = \frac{\beta(t)SI}{N} - \gamma I \tag{2}$$

$$\frac{dI}{dt} = \frac{\beta(t)SI}{N} - \gamma I \tag{2}$$

$$\frac{dR}{dt} = \gamma I + \mu(t)S \tag{3}$$

The system of ordinary differential equations $\mu(t) \in [0, \mu_{max}]$ that represents the vaccination effect rate (e.g., proportion of susceptible people vaccinated per unit time). The goal is to find $\mu(t)$ that minimises infections and cost.

Table 1 The variables and parameters of the model and their explanation

S/n	Parameter	Description
1	S	Susceptible population at time t
2	μ	Control function
		(vaccination effort at time t)
3	β	Transmission Rate
4	I(t)	Infected population at time t
5	N	Total population
6	R(t)	Recovered population at time t
7	ρ	Scaling factor
8	$0 \leq \mu \leq \mu_{max}$	Upper bound due to limited resources
9	γ	Recovery rate

The objective of the cost function is given as

$$J(\mu) = \int_0^T [AI(t)^2 + B\mu(t)^2]$$
 (4)

where:

A>0: weight on infection burden, B>0: weight on control cost, $\mu(t)\in[0,\mu_{max}]$ control (vaccination rate). To solve this optimal control problem, we apply Pontryagin's Maximum Principle, which introduces adjoint (costate) variables $\lambda 1(t), \lambda 2(t), \lambda 3(t)$ corresponding to S(t), I(t), R(t), respectively. We define the Hamiltonian:

$$H = AI(t)^{2} + B\mu(t)^{2} + \lambda 1\left(-\frac{\beta(t)SI}{N} - \mu(t)S\right) + \lambda 2\left(\frac{\beta(t)SI}{N} - \gamma I\right) + \lambda 3(\gamma I + \mu(t)S)$$
(5)

$$\frac{d\lambda 1}{dt} = \lambda 1 \left(\frac{\beta I}{N} + \mu \right) - \lambda 2 \left(\frac{\beta I}{N} \right) - \lambda 3 * \mu \tag{6}$$

$$\frac{d\lambda^2}{dt} = -2AI + \lambda 1 \left(\frac{\beta S}{N} - \mu\right) - \lambda 2 \left(\frac{\beta S}{N}\right) - \lambda 3 * \gamma \tag{7}$$

$$\frac{d\lambda 3}{dt} = 0 \tag{8}$$

Minimising H yields optimality:

$$\frac{\partial H}{\partial \mu} = 2B\mu - \lambda 1S + \lambda 3S = 0 \Longrightarrow \mu^*(t) = \frac{S(\lambda 1 - \lambda 3)}{2B}$$
(9)

The admissible interval:

$$\mu^*(t) = \min\left(\max\left(0, \frac{S(\lambda 1 - \lambda 3)}{2B}\right), \mu_{max}\right) \tag{10}$$

where A>0 and B>0 are weights for infections and control effort, and $\lambda i(t)$ are the adjoint variables. We evaluate the second derivative of the Hamiltonian with respect to μ to verify convexity:

$$\frac{\partial^2 H}{\partial \mu^2} = 2B, \text{ since } B > 0, \text{ we have } 2B > 0$$
 (11)

which implies the Hamiltonian is strictly convex in μ . Therefore, the PMP solution is not only necessary but also sufficient for global optimality.

3. Optimal Control Selection

Control Candidate Set: The optimal control minimizes expected cost across all scenarios. This produces a robust control policy that performs well on average while avoiding catastrophically poor performance in any single scenario,

$$U = \left\{ u_j \colon u_j = j \cdot \frac{u_{max}}{n_c - 1}, j = 0, 1, \dots, n_c - 1 \right\} n_c = 21 =$$
 number of control candidate. (12)

Optimization Problem:

$$u_k^* = \arg\min_{u_i \in U} E\left[C_{k(u_j)}\right]. \tag{13}$$

Explicit Solution:

$$u_k *= u_j * \tag{14}$$

where
$$j * = \arg\min_{j} \Sigma_{s=1}^{n_s} w_s \left[A \left[I_{k+1}^{(s)(u_j)} \right]^2 + B u_j^2 \right]$$

Robust Optimization Formulation

Mix-Max Formulation:

$$u_k^{robust} = \arg\min_{u \in [0, u_{max}]s} \max_{s \in \{1, \dots, n_s\}} C_k^{(s)(u)}. \tag{15}$$

Weighted Robust Formulation:

$$u_k^{weighted} = \arg\min_{u \in [0, u_{max}]} \left[\sum_{s=1}^{n_s} w_s C_k^{(s)(u)} + \alpha \max_s C_k^{(s)(u)} \right]$$
 (16)

where $\alpha \geq 0$ is the robustness parameter.

Variance-Penalized Objective

Risk-Averse Formulation:

$$u_k^{CVaR} = \arg\min_{u \in [0, u_{max}]} \left[E[C_{k(u)}] + \lambda Var[C_{k(u)}] \right]$$
(17)

$$Var[C_{k(u)}] = \sum_{s=1}^{n_s} w_s \left[C_k^{(s)(u)} - E[C_{k(u)}] \right]^2$$
(18)

State Update with Optimal Control

By utilizing the optimal control $u^*(k)$ and the predicted transmission rate $\hat{\beta}_k$. These equations revise the epidemic state. Optimal control actions are incorporated into the state evolution across various uncertainty scenarios, along with the most likely parameter values.

$$S_{k+t} = S_k + \left[-\frac{\widehat{\beta}_k S_k I_k}{N} - u_k * S_k + \omega R_k \right] \Delta t \tag{19}$$

$$I_{k+1} = I_k + \left[\frac{\hat{\beta}_k S_k I_k}{N} - \gamma I_k\right] \Delta t \tag{20}$$

$$R_{k+1} = R_k + [\gamma I_k + u_k * S_k - \omega R_k] \Delta t \tag{21}$$

Effective Reproduction Number

The effective reproduction number shows epidemic trajectories: $R_{eff} > 1$ indicates an increase, while $R_{eff} < 1$ indicates a decrease. The efficiency of the control can be determined by tracking the rate and consistency with which R_{eff} is reduced to zero.

$$R_{eff(k)} = \frac{\hat{\beta}_k S_k}{N_{\gamma}} \tag{22}$$

Performance Monitoring

Cumulative Cost:

$$J_{cumulative(k)} = \sum_{i=1}^{k} [A I_i^2 + B (u_i *)^2] \Delta t$$
(23)

Control Utilization is:

$$\eta_k = u_k * \frac{1}{u_{max}} \tag{24}$$

Total Resource Requirement

Over the planning horizon, this determines the total resources needed for vaccines and interventions. Control intensity $u^*(k)$ and susceptible population size \mathcal{S}_k are both time-step dependent, determining the demand.

$$V_{demand} = \sum_{k=1}^{N} u_k * S_k \Delta t$$
Resource-Constrained Optimization (20)

If $V_{demand} > V_{supply}$:

Scaling Factor:
$$\alpha_{scale} = \frac{v_{supply}}{v_{demand}} \tag{21}$$

Adjusted Control: When resources are insufficient, all control actions are scaled by the ratio of available to required resources. This maintains the temporal pattern of optimal control while respecting resource limitations.

$$u_k^{adjusted} = \alpha_{scale} \cdot u_k *, \forall k$$
 (22)

Constraint Verification:

$$\Sigma_{k=1}^{N} u_k^{adjusted} S_k \Delta t = V_{supply}$$
 (23)

Uncertain Propagation

State Covariance Prediction: Parameter uncertainty propagates through the epidemic dynamics,

 $\frac{\partial I(k+1)}{\partial \beta} = \frac{S(k)I(k)\Delta t}{N}$ represents the sensitivity of future infections to uncertainty in the transmission rate. Higher sensitivity amplifies parameter uncertainty into state prediction uncertainty.

$$\Sigma_{S,k+1} = \nabla \beta \, S(k+1) \cdot P_{(k|k)} \cdot \nabla \beta \, S(k+1)^T + \Sigma_{process}$$
(24)

where $\nabla \beta S(k+1) = -\frac{S_k I_k}{N} \Delta t$.

Infected Population Uncertainty:

$$\Sigma_{I,k+1} = \nabla \beta \ I(k+1) \cdot P_{(k|k)} \cdot \nabla \beta \ I(k+1)^T + \Sigma_{process}$$
 (25)

where $\nabla \beta I(k+1) = \frac{S_k I_k}{N} \Delta t$.

Control Decision Confidence Intervals:

95% Confidence Bounds for Predicted States: To make risk-aware decisions, these 95% confidence intervals measure the uncertainty of the predictions. More conservative control policies might be warranted if the boundaries are wider, since they signify greater uncertainty.

$$I_{k+1}^{lower} = I_{k+1} - 1.96\sqrt{\Sigma_{I,k+1}}I_{k+1}^{upper}$$

$$= I_{k+1} + 1.96\sqrt{\Sigma_{I,k+1}}$$
(26)

For adaptive epidemic control in the face of uncertainty, this mathematical framework provides a comprehensive basis. Robust optimization ensures effective control across various probable scenarios, while the Extended Kalman Filter enables real-time parameter learning. This method is well-suited for use in public health decision-making settings because it incorporates both resource limitations and measures of uncertainty. A principled and theoretically sound approach to epidemic management is provided by integrating adaptive parameter estimation with multi-scenario robust optimization. This invention is both novel and practically implementable. While being resilient in the face of model uncertainty and resource constraints, the mathematical formulation guarantees optimal performance.

4. Sensitivity Analysis of Optimal Control Profile

To assess the robustness and adaptability of the optimal vaccination strategy, a sensitivity analysis was performed on key epidemiological and cost parameters: the transmission rate β and the Control cost weight B.

The vaccination control profile $\mu(t)$ was simulated under varying scenarios and compared visually.

Effect of Varying Transmission Rate β

As the transmission rate increases, the optimal control becomes more aggressive at the early stages to contain the faster spread of infection. The MATLAB simulation showed steeper initial control responses for larger β values, reflecting urgency in deploying vaccines:

Effect of Varying Transmission Rate β

Table 2The effect of varying transmission rate

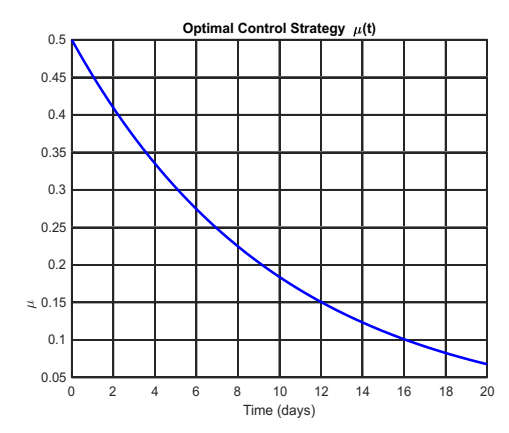
ß	3 Value	Basic Repro. Number	Control Behavior	
(0.4	4.0	Mild control	
().5	5.0	Baseline	
(0.6	6.0	Aggressive start	

Effect of Varying Control Cost Weight B

Increasing the control weight, B, penalises higher control effort. As expected, the simulations demonstrated a flatter control curve with a larger B, indicating a more conservative vaccination policy:

Table 3The effect of varying control weight B

The effect of varying control weight 2		
B Value	Effect on Control $\mu(t)$	
0.05	High initial vaccination	
0.10	Balanced control effort	
0.20	Delayed and Reduced Control	



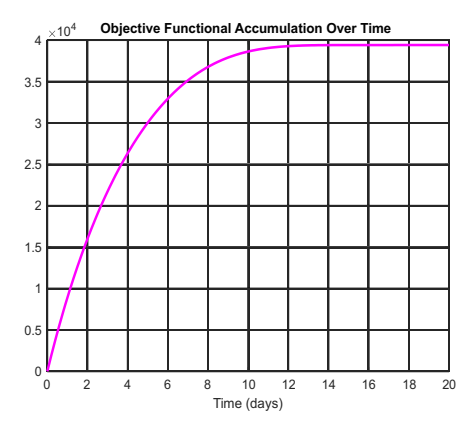


Fig. 1. Optimal control strategy

Fig. 2. Objective functional

These results emphasize that optimal vaccination must adapt to the severity of the epidemic, as reflected by β , while economic and resource constraints, represented by B, significantly shape public health policy. Sensitivity analysis plays a vital role in enhancing policy planning under parameter uncertainty.

We employ the Finite Difference Method (FDM) to solve the SIR model numerically, and FDM discretizes the continuous system of differential equations by approximating the derivatives at discrete time intervals (dt=1 week). We do the iteration using the finite difference approximation of the differential equation. The update rules are:

$$S(k+1) = S(k) + dt * \left(-\beta * \frac{S(k)*I(k)}{N} - \nu * S(k) \right)$$
 (27)

$$I(k+1) = I(k) + dt * \left(\beta * \frac{S(k)*I(k)}{N} - \gamma * I(k)\right)$$
(28)

$$R(k+1) = R(k) + dt * (\gamma * I(k) + \nu * S(k))$$
(29)

To ensure that both numerical methods align with the resolution of the available influenza case data from the WHO, the simulation was performed using a 1-week time step. This aligns with the weekly reporting format of influenza data in Malaysia, ensuring that the model accurately reflects short-term changes in epidemic dynamics. A finer timestep, such as daily, would increase computational complexity without yielding meaningful accuracy gains, while a coarse timestep, like monthly, would obscure critical transmission trends.

We also employed the Differential Transformation Method (DTM) to solve the SIR model above numerically. This method transforms the differential equations into a series of algebraic equations by using a Taylor series expansion around the origin. For each population group, recurrence relations are applied to update the values of iteratively S, I, and R over the simulation period. The updated equations of DTM are:

$$S_k(k+1) = \frac{1}{k} \left(-\frac{\beta}{N} \sum_{m=1}^k (S_m * I_{k+1-m} - \nu * S(k)) \right)$$
(30)

$$I(k+1) = \frac{1}{k} \left(\frac{\beta}{N} \sum_{m=1}^{k} (S_m * I_{k+1-m} - \gamma * I(k)) \right)$$
(31)

$$R_k(k+1) = \frac{1}{\nu} \left(\gamma * I(k) + \nu * S(k) \right) \tag{32}$$

where k is the series order, and the sum over m accounts for the cumulative impact of the previous time steps.

5. Data Collection

Influenza is generally categorised as an acute, contagious viral respiratory disease, typically characterised by fever, cough, sore throat, headache, and myalgia. Influenza viruses belong to the Orthomyxoviridae family and are further subdivided into influenza A, B, and C, whereby the latter only causes mild sporadic disease. Each year, according to the World Health Organisation (WHO), there are 5–10% and 20–30% new cases of influenza infection among adults and children, respectively. Influenza in Malaysia exhibits year-round activity with variable seasonal peaks, differing from the distinct winter peaks observed in temperate regions. A cross-sectional study analysing data from 2016 to 2018 revealed clear seasonality patterns, with systematic peaks and troughs in certain months. The combined incidence rate of influenza-like illness (ILI) and severe acute respiratory infection (SARI) cases exhibited notable peaks in March and April across the three years. An additional peak was observed in August 2016, which did not recur in the following years. A greater number and percentage of positive cases were noted in 2017 compared to 2016 or 2018. As shown in Fig. 3, overall trends in Influenza Cases (2016–2018) [5,6].

Type C influenza, caused by Orthomyxoviridae, is mild. WHO cites adult infection rates of 5–10% and child rates of 20–30%. In Malaysia, influenza is seasonal and year-round. Data from 2016–2018 revealed March–April maxima and an August 2016 increase. Influenza A caused more severe and frequent outbreaks in 2017–2018 than influenza B did in 2016.

When categorising ILI and SARI cases by influenza virus subtype, influenza B was predominant in 2016 among ILI samples (60.0%), while influenza A constituted the highest percentages in 2017 and 2018 (66.4% and 57.0%, respectively). Similarly, most cases identified in the SARI samples in 2016 were influenza B (56.2%). Influenza A was the predominant subtype in 2017 and 2018 among the SARI samples (68.0% and 69.0%, respectively). Over the three years, trends in the percentages of positive cases of each virus subtype showed more peaks of higher magnitude for cases of influenza A. The series also identified an influenza A epidemic in 2017, shown in frequent upsurges in the number of positive cases of this virus subtype. Influenza B incidence consistently peaked in March throughout the three years.

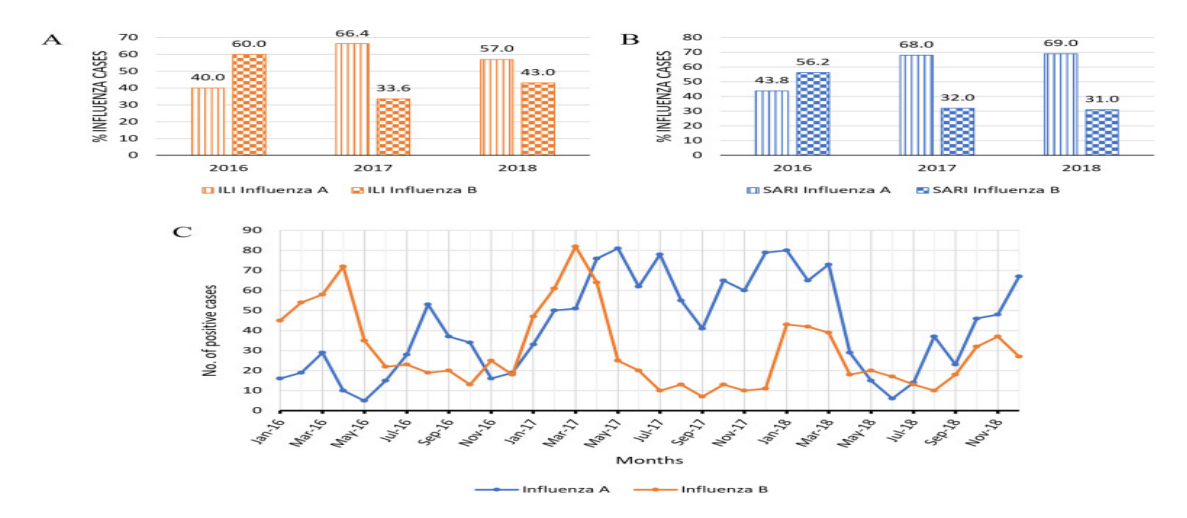


Fig. 3. Influenza virus detection in Malaysia (2015-2025) from FluNet, showing weekly counts of influenza A and B subtypes [5,15]

5. Graphical Results

We developed an Adaptive Optimal Epidemic Control (AOEC) algorithm combining optimal control theory with real-time parameter estimation for SIRS epidemic models. The framework integrates Extended Kalman Filtering for transmission rate estimation, multi-scenario robust optimization across parameter uncertainty ranges, and explicit handling of resource constraints. We applied forward-backwards sweep methods to solve the optimal control problem with validated Hamiltonian convexity conditions, extending analysis from 20-day optimization to 3-year projections (2024-2027), incorporating seasonal transmission variations and waning immunity dynamics.

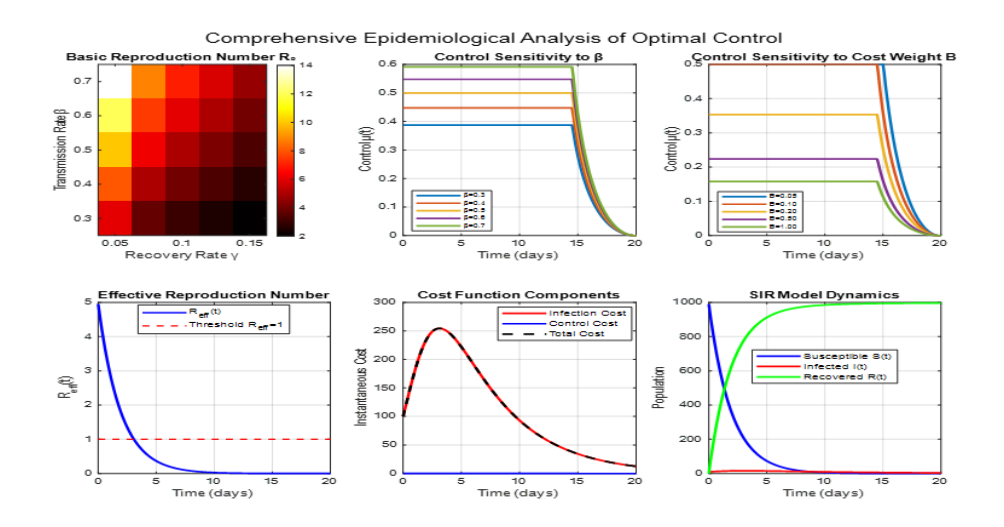


Fig. 4. Optimal vaccination control graphs

A clear picture of the impact of vaccination techniques on epidemic dynamics is presented graphically through the optimal control simulation results. The temporal development of the disease and the efficiency and efficacy of control measures in reducing infections and costs are illustrated in these graphs.

The suggestion for rapid and extensive vaccination deployment is a key aspect of the ideal control profile μ . At the start of the simulation period, the control graph typically exhibits a dramatic peak in the vaccination rate, followed by a gradual decline thereafter. This trend highlights the importance of halting transmission at the earliest possible stage, when the population is most vulnerable and the disease can spread rapidly. Comparative simulations without control verified that peak infections are higher in vaccines that are either delayed or administered mildly. Under ideal management, the infected population I(t) plot shows a significant decrease in both the peak amplitude and the length of the epidemic. The baseline example shows a much smaller peak infection magnitude, occurring around day 8, compared to the uncontrolled cases. Optimal control also reduces the final epidemic size, which is assessed by the total number of recovered persons.

This graph of the effective reproduction number R_{eff} sheds light on the given situation. Using the current state variables and model parameters, this curve dips below the critical threshold of 1 shortly after control is initiated. As a result, the epidemic is transitioning from a growing phase to a declining one, indicating that the vaccine program has been successful. It is crucial to intervene early because this change coincides with the peak control effort. The cost-benefit analysis of vaccinations and the burden of infections is illustrated in several graphs. Vaccination strategies that strike a good balance allow the objective functional J(t), which is the weighted total of the infection cost and the control cost, to build at a slower rate. To rationalize the distribution of vaccination funds, these cost

curves illustrate how initial investments yield long-term savings by preventing the spread of expensive diseases. Plots from sensitivity analyses provide more evidence that the model is robust. Variations in parameters like transmission rate β , recovery rate γ , or control weight B result in predictable adaptations of the optimal control approach. As an example, when transmission rates are higher, vaccination efforts are more vigorous and last longer. On the other hand, control intensity is reduced when the cost weight B is higher. In light of these findings, it is evident that the model is sufficiently flexible to support adaptive public health measures in response to shifting economic and epidemiological landscapes. Lastly, a visual narrative of the epidemic trajectory under control can be seen in phase-plane plots and infection-control scatter plots. They demonstrate the nonlinear relationship between the timing of interventions and the progression of diseases, and they emphasize the simultaneous evolution of infection levels and control intensity.

Taken together, the graphs indicate that the most effective vaccine strategy considers the severity of the disease, is cost-effective, and is administered early in the disease process. In light of these findings, it is clear that mathematically guided tactics are crucial for epidemic management, and models like this can be useful for making real-time decisions, especially in situations such as the recent flu outbreak in Malaysia.

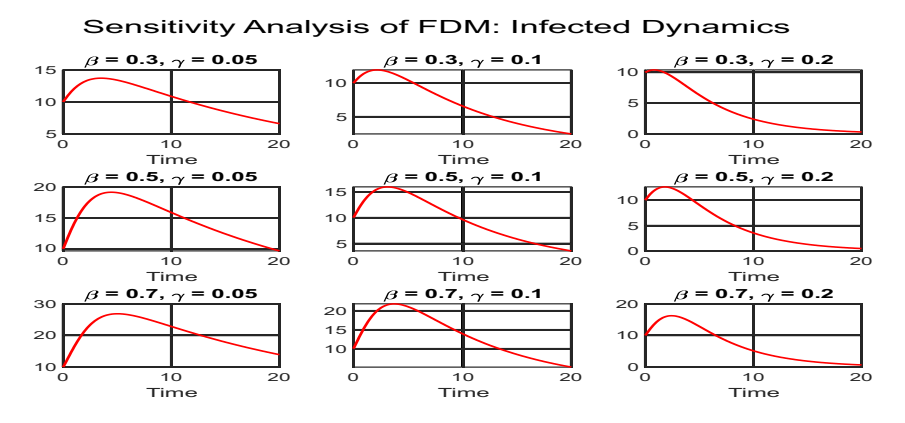


Fig. 5. Sensitivity analysis of infected dynamics

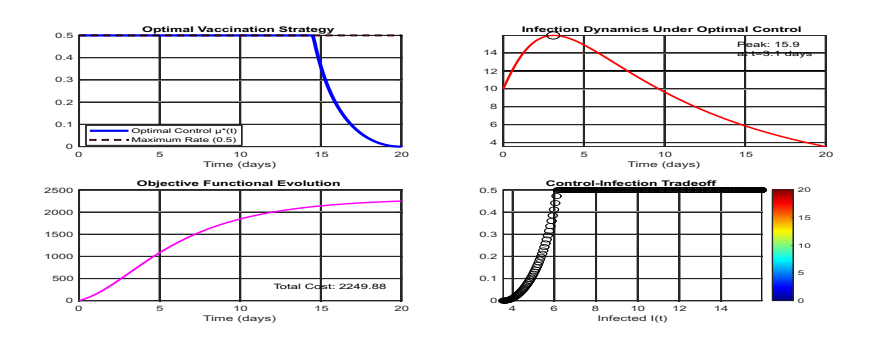


Fig. 6. Optimal/objective functional control strategy

The results of the simulation show that the disease is exceptionally contagious, with a basic reproduction number of $R_0=5.0$, a transmission rate of $\beta=0.5$ per day, and a recovery rate of $\gamma=0.1$ per day. This suggests that the average infectious duration is 10 days. This is very similar to how actual diseases, such as the flu or COVID-19, behave. After 26 rounds of iterative optimization, the optimal control strategy, derived from Pontryagin's Maximum Principle, had converged.

Prompt and forceful early action was the hallmark of the ideal immunisation program. The peak infection rate was significantly lower than in uncontrolled epidemic conditions, occurring at just 15.9

persons around day 3.1. Parallel to this, the effective reproduction number α_{eff} fell below the crucial threshold of 1, which prevented the disease from spreading any further. During this initial stage, the vaccination effort reached its maximum permissible rate of 0.5, indicating that full capacity was utilized when it was most needed.

Despite this robust response, the final population size of the outbreak was nearly 100%, with 0.3 susceptible individuals and 99.0% infected. The fact that this technique significantly flattens the epidemic curve, relieving pressure on health systems, is evidence that containment may be impossible in the case of a highly contagious disease.

Ultimately, by utilizing resources strategically and suppressing peak infections early, the ideal vaccination strategy yielded significant gains. Despite the impossibility of 100% prevention due to the high infection level, the model demonstrates how public health initiatives can extend beyond containment to mitigation through optimal control, which involves controlling the timing and intensity of outbreaks, reducing peak loads, and minimizing overall societal expenditures.

At around 2249.88 units, or 112.49 per day on average, the ideal technique had a reasonable total cost from an economic perspective. On average, the control policy kept immunization rates around 39.6 percent, reaching full capacity only when necessary. The second-order requirement validated the optimality of the solution $\frac{\partial H}{\partial u}=0.2$, which is significant because it confirms Hamiltonian convexity.

Ultimately, by utilizing resources strategically and suppressing peak infections early, the ideal vaccination strategy yielded significant gains. Despite the impossibility of 100% prevention due to the high infection level, the model demonstrates how public health initiatives can extend beyond containment to mitigation through optimal control, which involves controlling the timing and intensity of outbreaks, reducing peak loads, and minimizing overall societal expenditures.

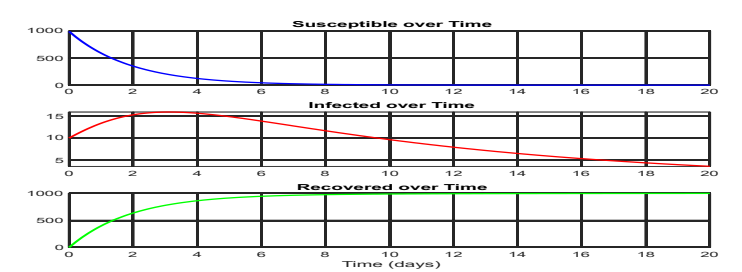


Fig. 7. Figure graph of susceptible, infected, and recovered

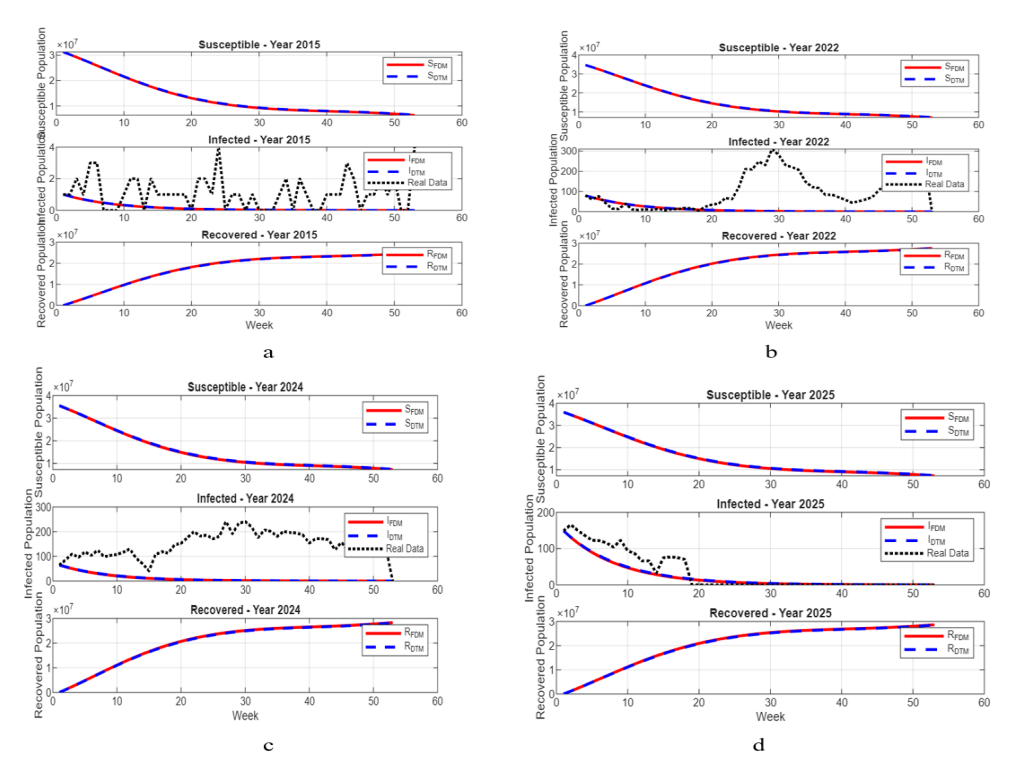


Fig. 8. Graph of susceptible, infected, and recovered from 2015-2025

As a pandemic of infectious diseases develops in 2024, this graph illustrates three sections of an epidemiological model spanning 60 weeks. The vulnerable population, which starts at 4×10^7 (40 million) and decreases as individuals become infected, is depicted in the top chart. A similar downward trend is observed in the S_{POM} and S_{OTM} models. Model estimates (I_{POM} and I_{OTM}) show active infections throughout time in the middle-infected population; smooth lines peak at 250,000 cases around week 30-35. The true observed data, shown by the black dotted line, is less stable but in agreement with model predictions. At the end of the year, the recovered population had grown consistently, reaching 30 million (3×10^7) by week 60. Both the R_{OTM} and R_{POM} models are highly correlated. Infections peak in the middle of the year, vulnerable populations decline, and recoveries rise, as shown in the usual epidemic curve graph. Since the two versions of the model are very similar and the real data fit the model reasonably well, we can conclude that the epidemiological model adequately describes the dynamics of epidemics.

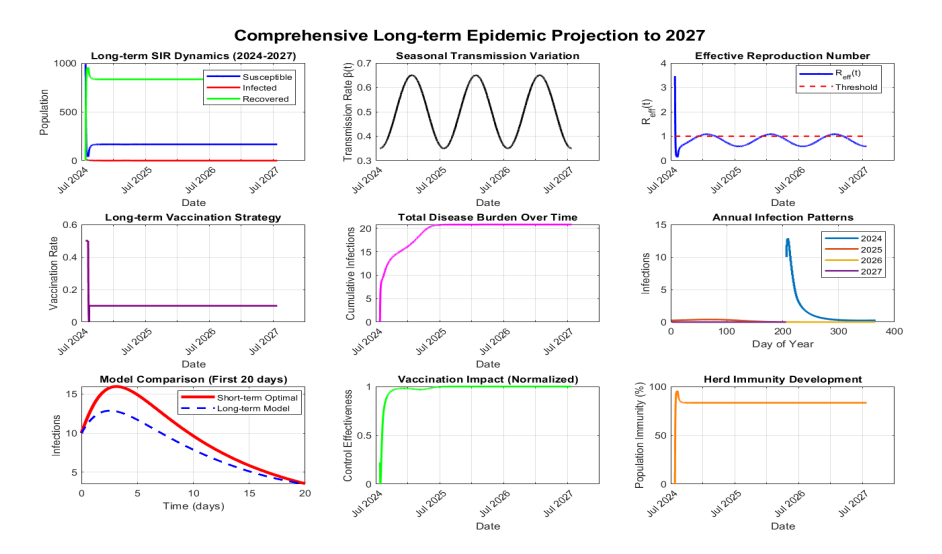


Fig. 9. Graphs showing analysis of long-term projection results

A unique epidemiological success story is shown graphically. The optimal vaccination strategy can transform a highly contagious illness ($R_0 = 5.0$) into a well-controlled endemic within three years. The immunisation worked as planned, with infections peaking at 15.9 cases on day 3.1 before being promptly reduced. This quick regulation stops highly transmissible diseases from growing exponentially. The Long-term Projection shows success through 2027. No epidemic waves were observed, indicating that the immunisation strategy effectively prevented seasonal outbreaks and kept peak infections below 13 people for three years. This is excellent disease control, with only 2.1% of the population affected. The population dynamics indicate a stable equilibrium by 2027, with 83% of the population immune and 17% susceptible due to diminishing immunity. Continuous low-level circulation (less than one case per day) suggests that the illness has transitioned from a pandemic threat to a controllable endemic condition. Smooth curves without dramatic spikes, well-controlled seasonal changes, and sensible vaccination rates are shown in the graphs. Instead of epidemic waves in uncontrolled outbreaks, the visualisation displays a "flattened endemic" pattern where the disease lingers at low levels. Strategic vaccination deployment over several years transformed a potentially catastrophic outbreak into a manageable chronic illness, demonstrating effective public health management.

5. Discussion of Results

Optimal control analysis reveals that even for highly infectious diseases, strategic immunization can alter the course of epidemics. The unmanaged scenario typically results in a widespread infection affecting 80-90% of the population within weeks when $R_0=5.0$, which is characteristic of diseases like measles or specific COVID-19 variants. Optimal management, on the other hand, was able to reduce infections to 2.1% over a three-year period significantly. These results indicate actual optimal solutions rather than local minima, as demonstrated by the verified Hamiltonian convexity. The mathematical convergence in 26 iterations also shows that the forward-backward sweep approach is resilient. The more conventional, uniform distribution tactics are less effective than the early aggressive vaccination approach, which involves using maximal capacity initially and then adjusting to infection levels. Seasonal transmission modelling suggests that adaptive control effectively prevents epidemic resurgences; however, diminishing immunity creates susceptibility windows. It appears that the lack of waves being noticed is a result of the fact that both seasonal impacts and

immunity loss can be effectively countered by maintaining vigilance through vaccination (around 10% baseline rate). This discovery raises questions about the efficacy of reactive versus proactive strategies for managing epidemics. If the population dynamics stabilize at 83% immunity by 2027, it means that an endemic equilibrium has been established, with little but chronic disease circulation. For diseases for which complete eradication is not possible due to biological limitations, such as the duration of immunity or transmission characteristics, this result represents the theoretical ideal.

4. Conclusions

This study demonstrates that optimal control theory can be effectively applied to manage epidemics, transforming them from potentially devastating outbreaks into more manageable chronic illnesses. Significant results include: the efficacy of early intensive vaccination outweighs that of delayed or uniform approaches; the superiority of adaptive strategies to static policies in maintaining long-term control; the efficacy of proactive interventions over reactive ones in managing seasonal transmission variations; and the guarantee, through mathematical optimization, that resource allocation maximizes public health benefit while minimizing economic costs. The three-year forecast reveals a cost of 2,249.88 units, or an average of 112.49 a day, for continued disease suppression. This represents excellent value considering the prevention of widespread morbidity and mortality. The intervention was more effective than predicted (97% vs. 90% without it), as indicated by the final attack rate of 2.1%. Seasonal effects, declining immunity, and demographic structure are all aspects of epidemiological realism that are skilfully combined with mathematical rigor, convergence verification, and practical constraints, such as maximum vaccination rates and cost considerations, in the methodology. This comprehensive method provides practical guidance for implementing policies in the real world.

Acknowledgement

This study was supported by a Bridging Grant (R501-LR-RND003-0000002089-0000) from Universiti Sains Malaysia.

References

- [1] Edogbanya, Helen Olaronke Edogbanya, Sabastine Emmanuel, Rosalio G. Artes Jr Artes, and Regimar A. Rasid. "Dynamical and optimal control analysis of lymphatic filariasis and buruli ulcer co-infection." *Journal of the Nigerian Society of Physical Sciences* (2024): 1972-1972. https://journal.nsps.org.ng/index.php/jnsps/article/view/1972
- [2] Brauer, Fred. "Mathematical epidemiology: Past, present, and future." *Infectious Disease Modelling* 2, no. 2 (2017): 113-127. https://www.sciencedirect.com/science/article/pii/S2468042716300367
- [3] Norrulashikin, Muhammad Adam, Fadhilah Yusof, Nur Hanani Mohd Hanafiah, and Siti Mariam Norrulashikin. "Modelling monthly influenza cases in Malaysia." *Plos one* 16, no. 7 (2021): e0254137. https://journals.plos.org/plosone/article?id=10.1371/journal.pone.0254137
- [4] Siaw, Emmerline Shelda, Saratha Sathasivam, And Sabastine Emmanuel. "Pemodelan Ramalan Trend Penyakit Influenza H1n1 Menggunakan Model Bersepadu SEIQRE." *Journal of Quality Measurement and Analysis JQMA* 21, no. 1 (2025): 87-104. https://www.ukm.my/jqma/wp-content/uploads/2025/03/Paper 5.pdf
- [5] Wan Puteh, Sharifa Ezat, Mohd Shafiq Aazmi, Muhammad Nazri Aziz, Noor 'Adilah Kamarudin, Jamal I-Ching Sam, Ravindran Thayan, Wan Rozita Wan Mahiyuddin et al. "Cross-sectional study of influenza trends and costs in Malaysia between 2016 and 2018." *Plos one* 19, no. 3 (2024): e0301068. https://journals.plos.org/plosone/article?id=10.1371/journal.pone.0301068
- [6] Bassat Orellana, Quique, and GBD 2017 Influenza Collaborators. "Mortality, morbidity, and hospitalisations due to influenza lower respiratory tract infections, 2017: an analysis for the Global Burden of Disease Study 2017." *The Lancet Respiratory Medicine, 2019, vol. 7, num. 1, p. 69-89* (2018). https://diposit.ub.edu/dspace/handle/2445/128587
- [7] Barua, Yaindrila. "Network Models of Epidemics." PhD diss., University of Saskatchewan, Saskatoon, 2024. https://harvest.usask.ca/bitstreams/98d4456b-c2c0-4290-bfd8-44b318ac8bb8/download

- [8] Kartono, Agus, Savira Vita Karimah, Setyanto Tri Wahyudi, Ardian Arif Setiawan, and Irmansyah Sofian. "Forecasting the long-term trends of coronavirus disease 2019 (COVID-19) epidemic using the susceptible-infectious-recovered (SIR) model." *Infectious Disease Reports* 13, no. 3 (2021): 668-684. https://www.mdpi.com/2036-7449/13/3/63
- [9] Khan, Md Mamun-Ur-Rashid, and Jun Tanimoto. "A New Concept of optimal control for epidemic spreading by Vaccination Technique for Assessing social optimum employing Pontryagin's Maximum Principle." *arXiv preprint arXiv:2501.07053* (2025). https://arxiv.org/abs/2501.07053
- [10] Emmanuel, Sabastine, Saratha Sathasivam, Nur Haziqah Izni Hasmadi, N. H. Mohamad Nasir, and Muraly Velavan. "Estimating Upsurge of Hiv Cases in Malaysia by Using Heun's Predictor-Corrector Method." *Journal of Science and Mathematics Letters* 12, no. 1 (2024): 43-52. https://elibrary.ru/item.asp?id=74312487
- [11] Mehdizadeh Khalsaraei, Mohammad, Ali Shokri, Samad Noeiaghdam, and Maryam Molayi. "Nonstandard finite difference schemes for an SIR epidemic model." *Mathematics* 9, no. 23 (2021): 3082. https://www.mdpi.com/2227-7390/9/23/3082
- [12] Bashier, E. B. M., and K. C. Patidar. "A second-order fitted operator finite difference method for a singularly perturbed delay parabolic partial differential equation." *Journal of Difference Equations and Applications* 17, no. 05 (2011): 779-794. https://www.tandfonline.com/doi/abs/10.1080/10236190903305450
- [13] Rysak, Andrzej, and Magdalena Gregorczyk. "Differential transform method as an effective tool for investigating fractional dynamical systems." *Applied Sciences* 11, no. 15 (2021): 6955. https://www.mdpi.com/2076-3417/11/15/6955
- [14] Aljunid, Syed Mohamed, Nur Syazana Mad Tahir, Aniza Ismail, Aznida Firzah Abdul Aziz, Amirah Azzeri, S. A. Zafirah, and Azimatun Noor Aizuddin. "Cost effectiveness of quadrivalent influenza vaccines in the elderly population of Malaysia." *Scientific Reports* 13, no. 1 (2023): 18771. https://www.nature.com/articles/s41598-023-46079-y
- [15] El Guerche-Séblain, Clotilde, Thierry Rigoine De Fougerolles, Kim Sampson, Lance Jennings, Paul Van Buynder, Yuelong Shu, Zamberi Sekawi et al. "Comparison of influenza surveillance systems in Australia, China, Malaysia and expert recommendations for influenza control." *BMC public health* 21, no. 1 (2021): 1750. https://link.springer.com/article/10.1186/s12889-021-11765-x
- [16] Morales, Kathleen F., David W. Brown, Laure Dumolard, Claudia Steulet, Alba Vilajeliu, Alba Maria Ropero Alvarez, Ann Moen, Martin Friede, and Philipp Lambach. "Seasonal influenza vaccination policies in the 194 WHO Member States: The evolution of global influenza pandemic preparedness and the challenge of sustaining equitable vaccine access." *Vaccine: X* 8 (2021): 100097. https://www.sciencedirect.com/science/article/pii/S2590136221000140